NUCL SCI TECH (2017) 28:46
DOI 10.1007/s41365-017-0208-9

Thermal analysis and tests of W/Cu brazing for primary collimator scraper in CSNS/RCS

Jie-Bing Yu[1,2] · Jia-Xin Chen[1,2] · Ling Kang[1,2] · Jie-Feng Wu[3] · Yi-Qing Zou[1,2]

Received: 25 November 2015 / Revised: 23 May 2016 / Accepted: 29 May 2016 / Published online: 27 February 2017

Abstract To the transverse beam collimation system in a rapid cycling synchrotron, an important component is the primary collimator, which improves emittance of the beam halo particles such that the particles outside the predefined trajectory can be absorbed by the secondary collimators. Given the material properties and power deposition distribution, the beam scraper of the primary collimator is a 0.17 mm tungsten foil on a double face-wedged copper block of 121.5 mm × 20 mm. The heat is transferred to the outside by a ϕ34 mm copper rod. In this paper, for minimizing brazing thermal stress, we report our theoretical analysis and tests on brazing the tungsten and copper materials which differ greatly in size. We show that the thermal stress effect can be controlled effectively by creating stress relief grooves on the copper block and inserting a tungsten transition layer into the copper block. This innovation contributes to the successful R&D of the primary collimator. And this study may be of help for working out a brazing plan of similar structures.

Keywords Scraper of primary collimator of CSNS/RCS · W/Cu brazing · Thermal analysis · Brazing tests

This work was supported by the National Natural Science Foundation of China (No.11375217).

✉ Jie-Bing Yu
yujb@ihep.ac.cn

1 Institute of High Energy Physics, Chinese Academy of Sciences, Beijing 100049, China

2 Dongguan Neutron Science Center, Dongguan 523803, China

3 Institute of Plasma Physics, Chinese Academy of Sciences, Hefei 230031, China

1 Introduction

The China Spallation Neutron Source (CSNS) consists of a negative hydrogen linac, a rapid cycling proton synchrotron (RCS) accelerating the beam to 1.6 GeV, a solid target station, and instruments for spallation neutron applications [1]. The transverse beam collimation system, with a primary collimator and four secondary collimators, is the key device in RCS. The halo particles, with increased emittance after scattering from the beam scraper in the primary collimator, are absorbed by the downstream secondary collimators after some phase shift [2, 3]. Different materials were studied as a candidate for scraper material by the physics department of CSNS. Tungsten, copper and tantalum materials impart a large scattering angle to the halo particles. They are of high melting point, good thermal conductivity, and a moderate price. From the three materials, tungsten is chosen to fabricate the primary collimator scraper, with a thickness of 0.17 mm [4, 5]. Thin and fragile, the tungsten slice is subjected to energy deposition by the particles. An extended power deposition heats the slice up, and an effective heat dissipation design is to weld the tungsten foil onto an oxygen-free copper block, which is connected to a ϕ34 mm copper rod that transfers the heat to cooling structure outside the vacuum chamber.

As shown in Fig. 1, the beam scraper of the primary collimator was designed as a 0.17 mm tungsten foil brazed on a double face-wedged copper block of 121.5 mm × 20 mm. Tungsten and copper differ greatly in thermal properties, especially, thermal expansion coefficient and thermal capacity (Table 1). It is hard to weld them together [6, 7], and the two materials of this structure contrast sharply in thickness, making the task even harder [8].

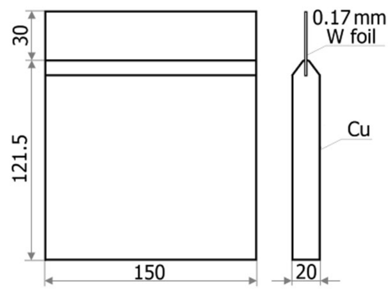

Fig. 1 Structure of the W/Cu assembly

Table 1 Thermal expansion coefficient (TEC) and specific heat capacity (SHC) of W and Cu

Materials	TEC (μm m^{-1} $°C^{-1}$)	SHC (J g^{-1} $°C^{-1}$)
Cu	16.4 (20–100 °C)	0.385
	18.5 (250 °C)	
	20.2 (500 °C)	
	24.8 (925 °C)	
W	4.4	0.134

The high thermal expansion ratio and large shrinkage during cooling cause great thermal stress, which tends to create brazing cracks [9]. Methods to minimize stress include: improving the structure technology, using brazing filler metals with the lowest possible fusion point, and inserting an adequate cushion layer between the base metals [10–22]. In Ref. [8], we found that the recrystallization temperature of a 0.17 mm tungsten foil was 1025 °C and the best brazing strength could be achieved by vacuum brazing technology, using Ag–Cu–Ti as brazing filling metals, and holding at 890 °C for 10 min. In this paper, we focus on minimizing W/Cu brazing thermal stress by improving the structure and inserting a transition layer, by finite elemental analysis (FEA) and experimental tests, toward a proper brazing and processing plan for heat treatment of the tungsten foil, which led to the successful acceptance of the primary collimator R&D.

2 Methods

To simplify the analysis, we did not consider plastic or brittle deformations, and effects of material welding, and just focus on reducing thermal stress by structure improvement and buffering inlet. Welding was simulated by a heat-up-to-cooling-down process of tungsten foil and copper block. Transient Thermal-Structural Coupled Analysis was utilized to obtain thermal stress in the cooling down process from welding temperature to room temperature.

The loading and constraint conditions of the analysis were:

1. Thermal loading: the copper block and tungsten foil were allowed to cool in vacuum, and temperature of the entire model dropped from 890 to 25 °C in 25 s and maintained at 25 °C for 5 s; and
2. Fixed loading: structural analysis was performed on the copper block bottom. As all the models were symmetrical about the XOY plane, to save computation time, half of the model was considered in the analysis and symmetrical constraints were applied to the plane of symmetry.

From the FEA results, a proper plan was established for test research so as to validate the reliability of analysis.

3 Improvement of the structure technology

As thermal stress is mainly concentrated on the joint, the tungsten foil is of minimal thickness, and tungsten material is hard and brittle, so there is little possibility of structural improvement at its joint structure. Therefore, structural improvement is only possible at the copper block joint.

The assembly consisting of different copper structures at the joint and the tungsten slice were analyzed. The temperature drop trends of all the models in the thermal analysis are shown in Fig. 2a. In 0–25 s, the temperature difference of the models remained basically the same, while in 25–30 s the temperature difference narrowed down to 0 °C. Figure 2b shows a typical analysis models and the constraint conditions. Temperature distribution at different seconds was treated as a loading in structural analysis and was introduced into the model. A fixed loading was applied to the bottom of the copper block. Figure 2c shows the maximum stress at different seconds for the model in Fig. 2b. The higher the minimum temperature is, the larger the temperature difference and the maximum stress of the model. Figure 2d shows the stress analysis results at 1.9 s loading time with the temperature distribution being used as transient structural analysis loading. The maximum stress fluctuates from the beginning and finally stabilizes around 400 MPa.

Figure 3 show stress distribution in the copper and the tungsten assembly for different copper structures at the joint under 2 ms loading corresponding to the same time point. It is clear from that the structural analysis located the maximum stress on the tungsten foil, on the joint to be specific. Different structures at the joint had considerable impact upon the stress distribution in the W/Cu assembly. The thermal stresses in Structures 3 and 4 were far less than those in Structures 1 and 2.

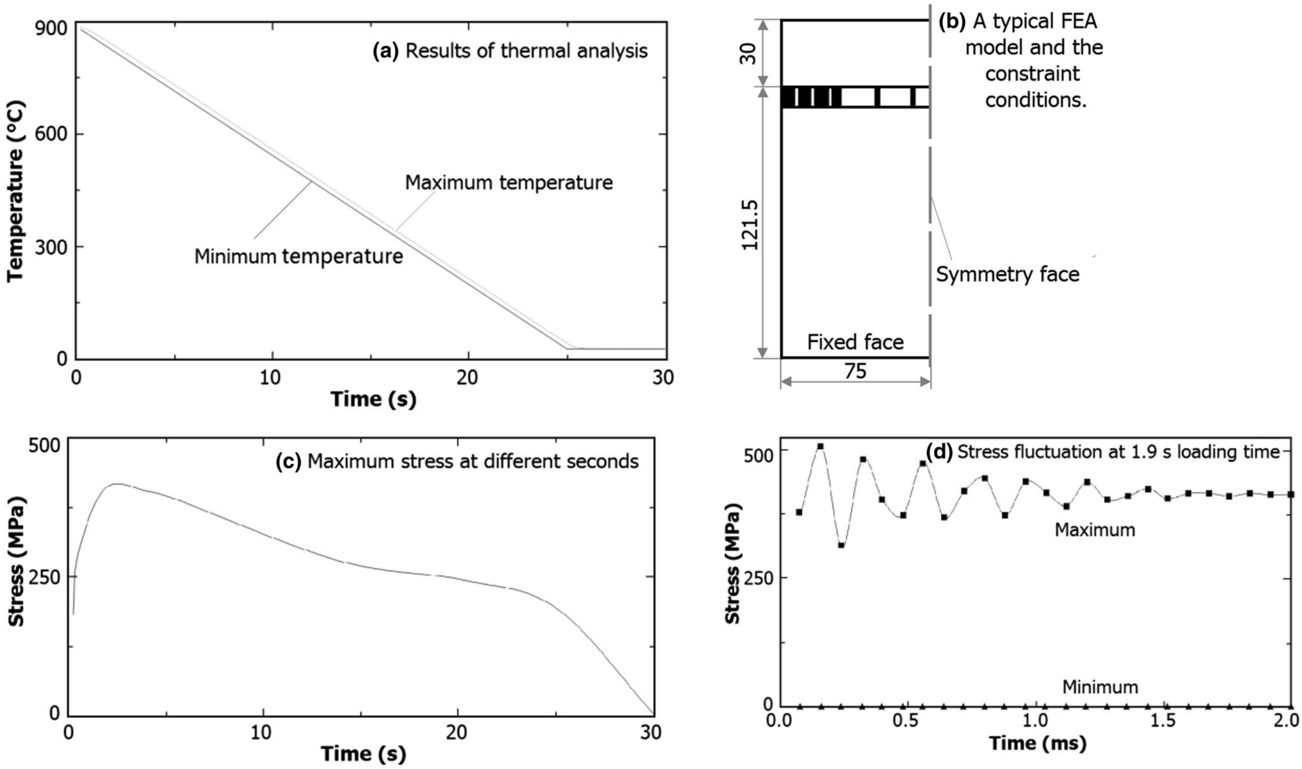

Fig. 2 Thermal and structural analysis results

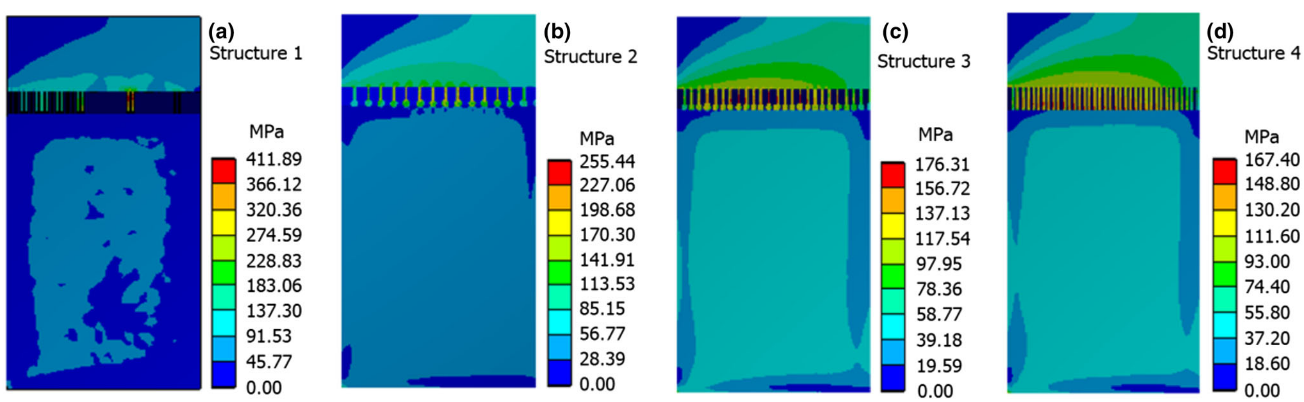

Fig. 3 Stress distribution in different copper structures at the joint and in the tungsten foil, under 2 ms loading at the same time point

To validate feasibility of the FEA, copper blocks of different structures were fabricated and welded with a 0.17 mm tungsten foil, as shown in Fig. 4. The double face-wedged head for tungsten foil welding was in structures of no grooves, fine grooves, nonuniform grooves, 1-mm groove in every 2 mm and 1-mm groove in every 3 mm.

We found that the W/Cu joint structure did have a great influence upon the W/Cu brazing quality. When the stress relief grooves were fine (Specimen b), no fold appeared on the tungsten foil, but less brazing wire was fused into the void between the tungsten and copper. The smaller the W/Cu contact area was, the poorer the brazing quality was. By changing structure and size of the stress relief groove, we had Specimens c, d and e, The brazing quality of Specimen c and d was somewhat improved, but the tungsten foil folded apparently; while a not-so-bad balance was achieved between the tungsten foil deformation and brazing quality of Specimen e. However, the small folds of tungsten foil could not meet CSNS's physics requirements. If a 0.17 mm tungsten foil was welded to a 20 mm copper block, the foil could hardly resist the shrinkage stress caused by the thermal expansion of the two materials. Improvement ought to be made by other methods.

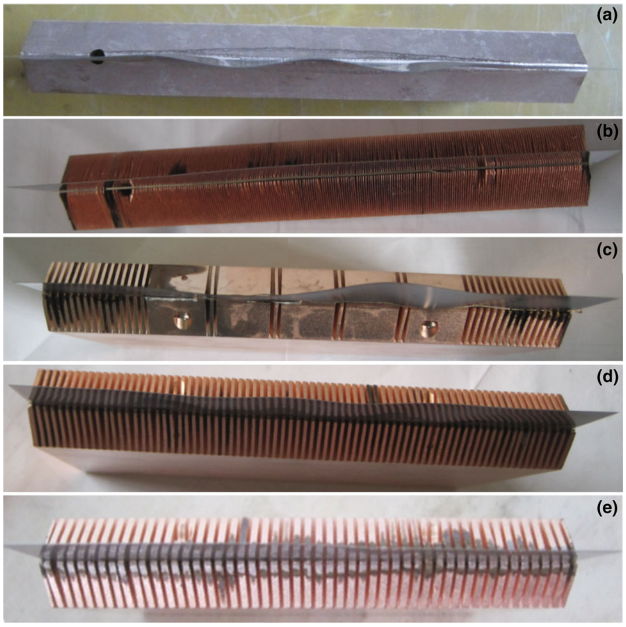

Fig. 4 Brazing test specimens of different copper structures. The double face-wedged head to weld with the tungsten foil was in structures of **a** no grooves, **b** fine grooves, **c** nonuniform grooves, **d** 1-mm groove in every 2 mm, and **e** 1-mm groove in every 3 mm

4 Insertion of a transition layer

To substantially reduce brazing stress in the tungsten foil, a transition layer has to be introduced in addition to the copper structure improvement. As two pieces of the same metals do not have the above brazing problems, the most reliable way to reduce the brazing stress in the tungsten foil is to weld a transition layer of tungsten sheet in suitable thickness on the copper block, and the transition layer was later welded with the tungsten slice. Based on this philosophy, tungsten sheets in different thicknesses

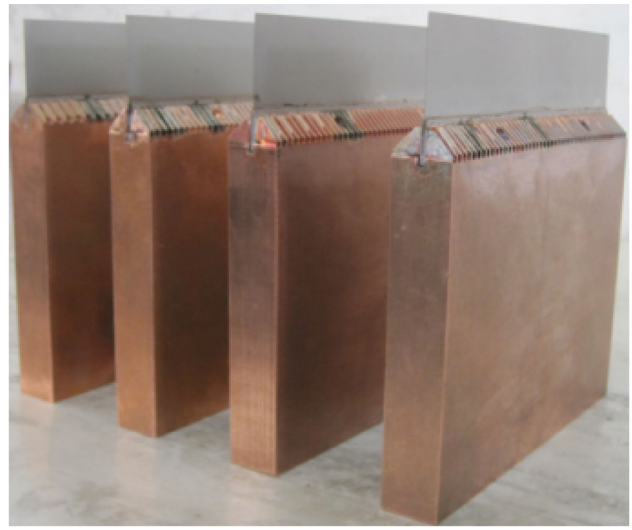

Fig. 6 W/Cu brazing specimens with a 2 mm tungsten transition layer

welded on copper blocks of the same structure were analyzed. The stress distributions of the general model with a transition tungsten sheet of 1.5 and 2 mm thick are shown in Fig. 5. Finite element analyses were performed on the assembly with the tungsten foil and a tungsten sheet of different thicknesses. With the sheet thicknesses of 1, 2 and 3 mm, the maximum stresses were 0.80, 0.87 and 1.65 MPa, respectively. So, when the tungsten sheets do not differ much in thickness, the thickness effect is small enough to be neglected.

Based on the FEA results, a brazing test was conducted. To ensure brazing quality of the tungsten foil, it was necessary to fabricate a number of grooves on the transition layer. This would be a tough machining task for the transition layer was too thin. Therefore, 2 mm tungsten sheet was used as the transition layer. The sheet was brazed with

Fig. 5 Analysis results of a copper structure with tungsten transition layer of different thicknesses, under 2 ms loading at the same time point

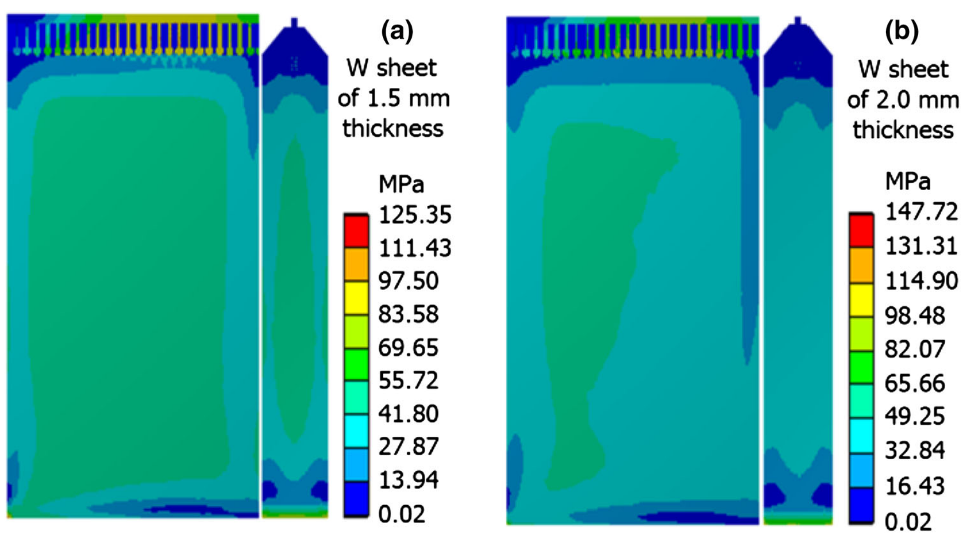

the copper block, grooves were machined on it, and the tungsten foil was brazed on the transition layer. Figure 6 shows the specimens of W/Cu brazing structure with a 2 mm tungsten transition layer. Brazing quality of the W/Cu structure with 0.17 mm tungsten foil well meets the physics requirements of the CSNS project.

5 Conclusion

We have explored on W/Cu brazing of large difference in size of the parts, and come up with a solution whereby the copper block structure is modified at the W/Cu joint and a tungsten transition layer of adequate thickness is inserted to cope with the problems of dissimilar metals and disparate thermal expansion coefficients. The feasibility of this plan has been validated by tests, ensuring the successful acceptance of the CSNS primary collimator. This study may be of help for developing a brazing plan for similar structures.

References

1. S. Wang, S.X. Fang, S.N. Fu et al., Introduction to the overall physics design of CSNS accelerators. Chin. Phys. C **33**(2), 1–3 (2009). doi:10.1088/1674-1137/33/S2/001
2. T. Wei, Q. Qin, Design of the two-stage collimation system for CSNS/RCS. Nucl. Instrum. Methods A **566**(2), 212–217 (2006). doi:10.1016/j.nima.2006.06.069
3. T. Wei, Q.B. Wu, W.Q. Li, Beam collimation for CSNS/RCS. Chin. Phys. C **34**(4), 506–511 (2010). doi:10.1088/1674-1137/34/4/018
4. Y.Q. Zou, L. Kang, H.M. Qu et al., Design and research of primary collimator for CSNS/RCS. High Power Laser Part. Beams **25**(3), 741–745 (2013). doi:10.3788/HPLPB20132503.0741
5. Y.Q. Zou, N. Wang, L. Kang et al., Thermal analysis and cooling structure design of the primary collimator in CSNS/RCS. Chin. Phys. C **37**(5), 05704 (2013). doi:10.1088/1674-1137/37/5/057004
6. C.P. Liang, J.L. Fan, H.R. Gong et al., Interface structure and work function of W–Cu interfaces. Appl. Phys. Lett. **103**(21), 211604 (2013). doi:10.1063/1.4833249
7. C.H. Chen, X.J. Liu, Z.B. Wang, The effects of joining methods on the resistivity of W-Cu alloy and Cu joint. Phys. Proc. **25**, 68–72 (2012). doi:10.1016/j.phpro.2013.03.051
8. Y.Q. Zou, L. Kang, J.B. Yu et al., Experiments and analysis of thin tungsten slice and W/Cu brazing for primary collimator scraper in CSNS/RCS. Sci. China Ser. G **57**(4), 1–4 (2014). doi:10.1007/s11433-013-5386-9
9. Y.J. Li, J. Wang, P. Liu, *Welding of Dissimilar Hard-to-Weld Materials and Its Application* (Chemical Industry Press, Beijing, 2004), pp. 36–38
10. W.B. Lee, B.D. Kwon, S.B. Jung, Effect of bonding time on joint properties of vacuum brazed WC_Co hard metal/carbon steel using stacked Cu and Ni alloy as insert metal. Mater. Sci. Technol. Ser. **20**(11), 1474–1478 (2004). doi:10.1179/026708304X4312
11. K. Suganuma, T. Okamoto, Y. Miyamoto et al., Joining Si3N4 to type 405 steel with soft metal interlayers. Mater. Sci. Technol. Ser. **2**(11), 1156–1161 (1986). doi:10.1179/mst.1986.2.11.1156
12. K. Loki, M. Nayama, S. Tsujimura et al., Development and heat load experiments of graphite brazed to stainless steel for the first wall structure of Fer. Fusion Eng. Des. **9**, 283–287 (1989). doi:10.1016/S0920-3796(89)80047-X
13. R.U. Vaidya, P. Rangaswamy, M.A.M. Bourke et al., Measurement of bulk residual stresses in molybdenum disilicide/stainless steel joints using neutron scattering. Acta Mater. **46**(6), 2047–2061 (1998). doi:10.1016/S1359-6454(97)00429-1
14. Q.S. Cai, W.S. Liu, Y.Z. Ma et al., Diffusion brazing of tungsten and steel using Ti–Ni liquid phase forming interlayer. Fusion Eng. Des. **91**(2), 67–72 (2015). doi:10.1016/j.fusengdes.2014.12.029
15. T. Zaharinie, R. Moshwan, F. Yusof et al., Vacuum brazing of sapphire with Inconel 600 using Cu/Ni porous composite interlayer for gas pressure sensor application. Mater Des. **54**, 375–381 (2014). doi:10.1016/j.matdes.2013.08.046
16. A.P. Xian, Z.Y. Si, Interlayer design for joining pressureless sintered sialon ceramic and 40Cr steel brazing with Ag 57 Cu 38 Ti 5 filler metal. J. Mater. Sci. **27**(6), 1560–1566 (1992). doi:10.1007/BF00542918
17. A. Elrefaey, W. Tillmann, Brazing of titanium to steel with different filler metals: analysis and comparison. J. Mater. Sci. **45**(16), 4332–4338 (2010). doi:10.1007/s10853-010-4357-z
18. Q. Han, Q.S. Wu, J.W. Chen et al., Analysis of fixation method of fuel assembly for lead-alloy cooled reactor. J. Nucl. Sci. Technol. **26**(5), 050601 (2015). doi:10.13538/j.1001-8042/nst.26.050601
19. L. Zhao, X.H. Li, J.B. Hou et al., Bonding of Cf/SiC composite to Invar alloy using an active cement, Ag–Cu eutectic and Cu interlayer. Appl. Surf. Sci. **258**(24), 10053–10057 (2012). doi:10.1016/j.apsusc.2012.06.073
20. X.G. Song, J. Cao, H.J. Chen et al., Contact reactive brazing of Ti53311S alloy using Cu foil as interlayer: interlayer microstructure and joining properties. Mater. Des. **46**, 895–901 (2013). doi:10.1016/j.matdes.2012.11.044
21. W.Q. Yang, T.S. Lin, P. He et al., Microstructural evolution and growth behavior of in situ TiB whisker array in ZrB 2—SiC/Ti6Al4V brazing joints. J. Am. Ceram. Soc. **96**(12), 3712–3719 (2013). doi:10.1111/jace.12629
22. H.G. Dong, Z.L. Yang, Z.R. Wang et al., Vacuum brazing TC4 titanium alloy to 304 stainless steel with Cu–Ti–Ni–Zr–V amorphous alloy foil. J. Mater. Eng. Perform. **23**(10), 3770–3777 (2014). doi:10.1007/s11665-014-1145-y